جامعة الملك عبدالله
للعلوم والتقنية
King Abdullah University of
Science and Technology

An Experimental and Numerical Approach for the Best Enhanced Oil Recovery Strategy in Capillary-Dominant Reservoirs

OTC-31602-MS

An Experimental and Numerical Approach for the Best Enhanced Oil Recovery Strategy in Capillary-Dominant Reservoirs

Ahmad Alabdulghani, Saudi Aramco; Hussein Hoteit and King Abdullah, University of Science and Technology, KAUST

 DOI 10.4043/31602-MS

This paper was prepared for presentation at the Offshore Technology Conference Asia held in Kuala Lumpur, Malaysia, 22 - 25 March 2022.

Abstract

Working with naturally fractured reservoirs (NFRs) can be challenging. Inadequate understanding of the enhanced oil recovery (EOR) driving forces in these reservoirs may result in serious conformance issues due to excessive water production. As a result, this work investigates and numerically validates some fundamental flow mechanisms in heterogeneous reservoirs, particularly capillary-dominant ones, to highlight the best EOR strategy for this specific case.

Consequently, a two-dimensional lab-scale reservoir model with injection and production ports was designed, fabricated, and tested in single-phase and two-phase flow scenarios, simulating a water-wet fractured system. First, a single-phase flow waterflood baseline was studied, compared to the literature, verified by commercial reservoir simulation software, and eventually considered to calibrate the porosity and permeability model in the simulation model where the controlling variables are limited. Based on this work, the same procedures were experimentally repeated and verified by simulation, where waterflooding and polymer injection were used to displace oil with more governing variables.

The single-phase scenarios aided in distinguishing between the waterflood and polymer flood cases. Water prefers to channel through high permeable streaks when injected into a fractured water-wet reservoir, resulting in poor volumetric sweep and significant bypassed zones. Whereas the controlling variables in two-phase flow were increased, capillarity and mobility ratio were dominant in the simulation. During waterflooding, flow divergence was observed faster toward the matrix medium, overriding the high permeability front in the fracture due to the strong capillarity contrast between the matrix and fracture media. Even when capillarity is strongly present, polymer flooding demonstrated a better volumetric sweep in all scenarios.

The unique demonstration of fluid flow inside the two-dimensional lab-scale reservoir model, as well as numerical simulation, shed light on the efficacy of these EOR strategies in fractured reservoirs. Furthermore, for the first time, the behavior of capillary-dominant reservoirs with an advancing flow path within smaller pores compared to larger ones within the reservoir media has been experimentally captured. Understanding reservoir characteristics and having the know-how to implement the best recovery scenario can, in fact, maximize the field's life cycle and increase the Recovery Factor (RF).

Introduction

Although carbonate reservoirs are abundant in hydrocarbon, the nature of the carbonate structure, texture, diagenetic processes, and the labyrinth of the pore network imposes a significant challenge to increase the RF. Moreover, most carbonate reservoirs are naturally fractured and can appear as fissures or even fracture swarms, complicating the understanding of fluid flow behavior (Burchette, 2012; Schlumberger Limited, 2008). Furthermore, rock wettability is another characteristic that complicates fluid flow. In contrast to sandstone reservoirs, which exhibit strong water-wet behaviors, most carbonate reservoirs are known to be mixed-wet. This combination of wettability makes the oil more difficult to extract. This mix in wettability makes the oil harder to extract as rocks prefer to imbibe oil (Hoteit & Firoozabadi, 2008; Schlumberger Limited, 2008).

Heterogeneity of Reservoirs

Because most reservoir rocks are heterogeneous, reservoir heterogeneity is of great interest to many scientists and engineers (Fanchi, 2006; Satter & Iqbal, 2016; Terry & Rogers, 2015). Heterogeneity can occur at various scales, ranging from microscopic to megascopic. It can take multiple forms, including changes in geological sequences, unconformities, rock grading variations, significant grain sorting differences, and the presence of channels, vugs, or fractures (Albattat & Hoteit, 2021; Hoteit, 2013; Satter & Iqbal, 2016). These variations have the potential to significantly impact reservoir performance and reserves. The implications of various heterogeneity forms in sandstone and carbonate reservoirs are listed in Table 1 (Satter & Iqbal, 2016).

Table 1—Lists the typical heterogeneity that occurs in sandstone and carbonate reservoirs, as well as its impact.

Reservoir	Type of Heterogeneities	Possible Impact
Sandstone	– Grain sorting variation – Existence of impurities – Presence of fractures	– Weakening the reservoir quality – Fractures can improve connectivity in tight formations
Carbonate	– Existence of lamination – Presence of fractures – Facies variation – Presence of vugs	– Improvement of production for a while – Complications in sweep efficiency and water breakthrough

Other complications include reservoir damage, uncertainty in determining reservoir boundaries, a dramatic drop in the production curve, difficulties in placing wells, additional costs for workover and completion, dealing with water and its associated problems, selecting the best EOR method, and many others (Satter & Iqbal, 2016). Dealing with heterogeneities can be challenging, requiring skills and knowledge of the field's geology and physics (Satter & Iqbal, 2016; Selley, 1985; Terry & Rogers, 2015). Therefore, collaborative efforts in formation evaluation, reservoir modeling, characterization, and simulation are being undertaken to maximize recovery. Nonetheless, experts rely extensively on interpreting core analyses and understanding the region's geology.

Implication of Fractures

Fractures are a type of complex heterogeneity in the reservoir. Therefore, dealing with them can be tricky. Fissures, cracks, veins, joints, cleavages, and faults are all examples of fractures (Selley, 1985). Thus, not all fractures are conductive and do not necessarily improve flow because they can be open or closed (Da Prat, 1990). Upscaling and modifying the permeability of the model may suffice to determine the actual impact of the fractures. Nonetheless, in a fractured heterogeneous reservoir, upscaling with too many uncertainties may not be the best solution (Narr et al., 2006; Da Prat, 1990).

Naturally Fractured Reservoirs (NFRs) are reservoirs with naturally occurring fractures that significantly impact porosity, permeability, production rate, and recovery (Narr et al., 2006; Nelson, 2001). Therefore, they differ considerably in many areas, including geology, geophysics, performance, and economics (Warren & Root, 1963). Nelson (2001) defined fractured reservoirs based on the impact of the fracture on porosity and permeability (He, Santoso, et al., 2021; He, Sinan, et al., 2021; Lyons et al., 2015; Nelson, 2001). The four types of fractures are summarized in Table 2 (Nelson, 2001).

Table 2—Summary of the four types of fractures.

Type	Description
1	Fractures dominate the reservoir porosity and permeability (no matrix contribution)
2	Fractures enhance the permeability while the matrix provides the higher percentage
3	Fractures support the permeability in an early stage of production
4	Fractures do not contribute to the overall porosity and permeability (no fracture contribution)

Due to strong-bond capillarity within the reservoir media, capillary-dominant reservoirs exhibit an advancing flow path in two-phase flow within smaller pores compared to the larger ones inside the reservoir. Inadequate understanding of the recovery mechanisms and reservoir heterogeneity may result in conformance issues and, hence, low RF (Al-Nakhli et al., 2016; Aublinger, 2015; Glasbergen et al., 2014; Shepherd, 2009).

Waterflooding (WF)

Following primary depletion in a conventional oil reservoir, flooding with water is the most advantageous option for increasing the RF by improving or maintaining reservoir pressure. It works by moving water as a fluid bank and pushing oil to maintain oil production and maximize recovery. Water was chosen because it is effective, abundant, relatively cheaper than any other fluid, quickly injected, and easily disposed of compared to other hazardous alternatives (Fanchi, 2006; Lake et al., 2014; Terry & Rogers, 2015).

The recovery efficiency varies from one field to the next. The main factors, however, are reservoir heterogeneities, wettabilities, and mobility ratios. The incremental increase in reservoir total recovery after implementing the waterflooding technique is depicted in Figure 1. Knowing that coping with early water breakthrough production can be avoided or delayed would make a massive difference in total RF (Almohsin et al., 2017; Bailey et al., 2000; Goudarzi et al., 2014).

Several factors influence the design of a waterflooding technique, including economics, field size, field location, spacing between wells, pattern selections, injection rate, lithology, reservoir quality, fluid properties, and others. Some indicators can predict the recovery ranges during the secondary recovery. It reveals a great deal about reservoir transmissibility and storage. The broad implementation of the waterflooding technique is not limited to pre-implementation evaluation and strategy durations. It is also a daily task monitoring and post-implementation evaluation, particularly in highly uncertain reservoirs due to heterogeneity. Furthermore, wettability is another characteristic that adds to the heterogeneity (Donaldson et al., 1985; Fanchi, 2006; Satter & Iqbal, 2016; Terry & Rogers, 2015).

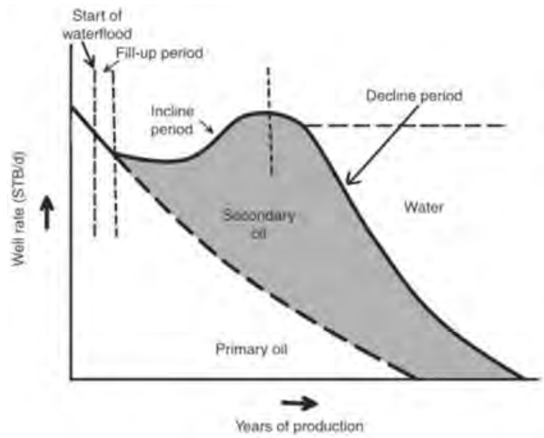

Figure 1—An image depicting the progressive growth of a successful waterflooding job.

Therefore, implementing water injection in fractured water-wet formation can be challenging because water prefers to channel through high permeable streaks at the strata's bed (Figure 2) (Satter & Iqbal, 2016; Sheng, 2011). Furthermore, waterflooding in heavy-oil reservoirs is not recommended because viscus fingering issues may arise due to the high mobility ratio, resulting in poor volumetric sweep efficiency, leaving large amounts of oil bypassed (Lyons et al., 2015; Sheng, 2011; Terry & Rogers, 2015).

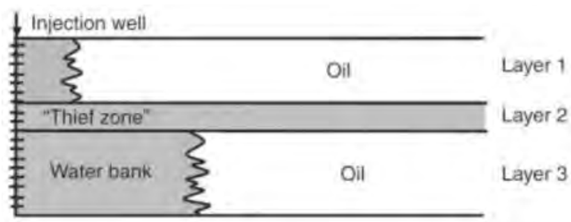

Figure 2—An illustration of the vertical sweep efficiency achieved by a waterflooding technique in a heterogeneous reservoir.

Chemical Enhanced Oil Recovery (CEOR)

Enhanced oil recovery can occur at any stage of the field's lifecycle, though most deployments occur during tertiary recovery. It can be accomplished by injecting fluids or gases that did not previously exist in the reservoir (Lake et al., 2014; Muggeridge et al., 2014). The most common EOR methods include thermal, Steam, And Gas Push (**SAGP**), miscible, microbial, and, most importantly, chemical flooding (Sheng, 2011).

Chemical flooding processes are the most effective and the future of conventional hydrocarbon recoveries, particularly in light and medium gravity oil. In terms of practice or implementation, it is similar to waterflooding processes. However, the execution details are dependent on the pill composition and the duration target. The CEOR's primary goal is to reduce the mobility ratio to improve sweep efficiency or reduce interfacial tension to improve displacement efficiency. CEOR contains a surfactant, polymer, micellar-polymer, alkaline flooding, and other ingredients. Chemical flooding typically necessitates a thorough reservoir evaluation and simulation prior to implementation. Furthermore, additional investments are required for downstream infrastructure, chemical supplies, and processing. Chemical flooding has several advantages, including increasing the recovery factor, speeding up the recovery, improving the sweep, and lowering the water cut.

Increasing the viscosity of the injected water by adding polymer would alter the mobility ratio and improve the volumetric sweep efficiency. Polymer flooding projects are well-developed and, by far, the most widely used CEOR strategy due to their low risk and applicability to a wide range of reservoir conditions. They are mixed with the injected water to form the polymer solution, determined by the polymer concentration, water salinity, reservoir temperature, and polymer molecular weight. The mobility ratio of the viscous polymer solution can be less than one (Sheng, 2011; Terry & Rogers, 2015).

Furthermore, polymer selection is a critical process that necessitates knowledge of the reservoir's petrophysical properties as well as the characteristics of the reservoir rocks. In some cases, the side effects of polymer injection can be severe and difficult to reverse (Hoteit et al., 2016; Sugar et al., 2021). It has the potential to reduce effective permeability, increase injection pressure, decrease well injectivity, and be absorbed by reservoir rocks. Polymer flooding is advantageous in reservoirs with high porosity and permeability. Furthermore, the vertical permeability should be adequate to allow the polymer to make sufficient contact with the reservoir heterogeneity without jeopardizing or violating the injection pressure threshold (Sheng, 2011; Terry & Rogers, 2015).

Methodology

Laboratory Model Design and Preparation

We designed a transparent 2D lab-scale model that will allow us to visualize heterogeneous porous media in a sandbox with injection and production ports that mimic wells. We chose to keep the sandbox as small as possible by placing one injection and one production port symmetrically at the corners. The sandbox measures 12×12×4.25 cm in total. Figure 3 depicts the design of model two with dimensions.

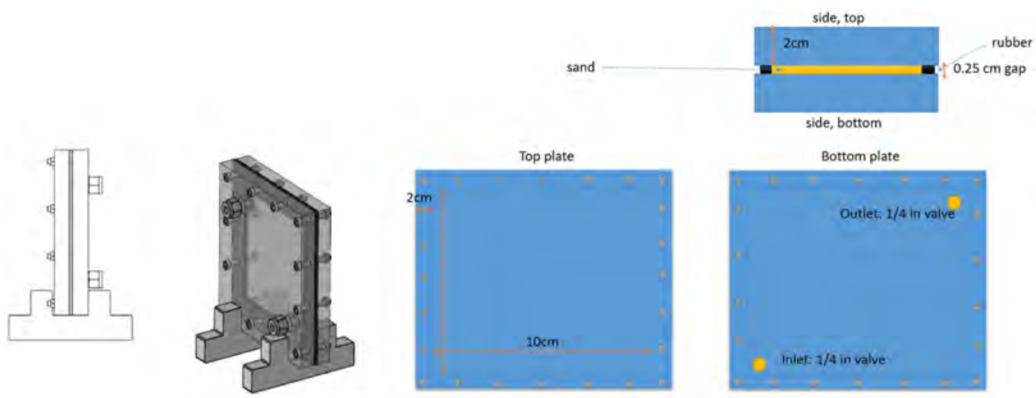

Figure 3—A sketch of the new sandbox model with the dimensions.

It comprises two transparent acrylic sheets, one on the front and one on the back. Each plate has 24 holes to securely tighten the sandbox with 24 screws to ensure that the acrylic sheets do not deform during any phase of the experiment. The middle layer is made of rubber and serves two functions: providing a cushion during nut tightening and housing the porous media. The porous media will be housed inside a measuring dimension of 10×10×0.25 cm. The bottom plate is perforated with two holes (0.25 inches each). The bottom one serves as an injection port and the top one as a production port, both of which are fitted with a Swagelok ball valve.

We used well-sorted silica sand for the porous media. Two types of silica sand were obtained for that purpose, both of which were water-wet porous media. The matrix of the porous media will be filled with medium class sand with a grain size of [0.42 to 0.71] mm, while the conductive fracture will be filled with very coarse class one with a grain size of [1.00 to 2.00] mm (Figure 4). The particle density is 2.67 g/cm^3 on average. The matrix porosity was found to be 32%, while the fracture porosity was 47%.

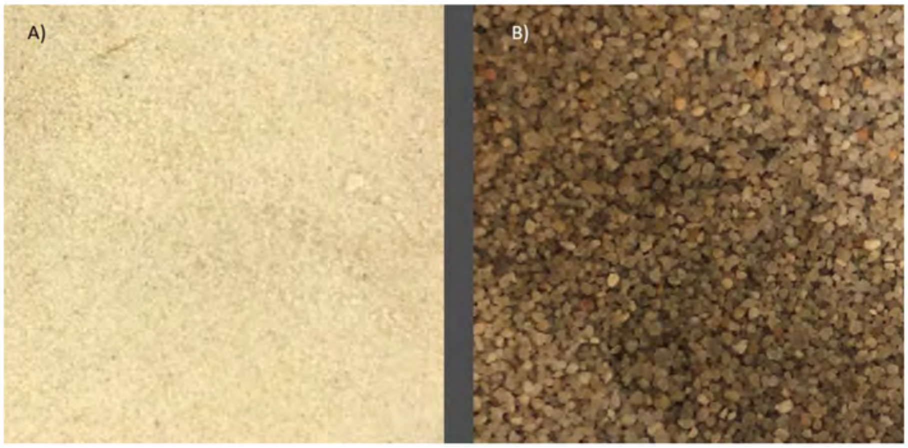

Figure 4—A photo on the left (A) depicts matrix grains, while the photo on the right (B) depicts fracture grains.

Fabricating and Testing the Sandbox

The model was created in the Core Labs at King Abdullah University of Science and Technology (KAUST). The system was tested and found to be functional. There were no water leaks or compaction issues discovered. The new sandbox requires about 25 mL of water to fill it. Because the dimension was compact and easy to handle, the filling process was simple. The sandbox was initially filled with matrix grains before being sprayed with water to ensure that no particle movement occurred during any process. The fracture was placed tangentially from the bottom left corner to the top right corner (Figure 5). The length and width of the high-permeability medium used to simulate a fracture are 7.00 cm and 2.00 cm, respectively.

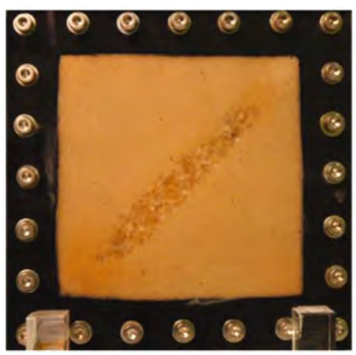

Figure 5—A photograph of the new sandbox model.

Equipment Setup

We used a nylon screen (53 µm mesh opening, 270 mesh size) to protect the outlet port from sand production. The goal is to conduct experiments with water or polymer injection in single-phase and two-phase flow scenarios. Therefore, we required fluids such as water, oil, and polymer. A tracer was used to create color contrast to visualize the fluid flow. We used treated water for the water and transparent light mineral oil with a viscosity of 30 cP for the oil. The 1000 ppm polymer solution was made with synthetic HPAM polymer powder and FLOPAAM 3330 S, which was filtered to remove impurities (Figure 6). This polymer solution is suitable for reservoirs with temperatures up to 70°C and TDS (Total Dissolved Solids) levels of up to 35,000 ppm, with a maximum of 1000 ppm divalent ions. FLOPAAM 3330 S has a low molecular weight and is anionic to a high degree.

Figure 6—A photo on the left (A) shows the polymer used to make the 1000 ppm polymer solution, while a photo on the right (B) shows the setup for filtering the impurities.

The other tool required is a pump. For that purpose, we used the Teledyne ISCO 500D syringe pump for water and polymer injection and the Teledyne ISCO 260D syringe pump for oil injection. A comparison of the two models is shown in Table 3. The pumps can be set to run at either constant flow or constant pressure. A constant flow rate will suffice for the purposes of our experiment. The pumps were connected to the sandbox via a 0.25-inch translucent plastic tube, with another tube connecting the outlet port to the drainage system.

Table 3—A comparison between the specifications of a water and polymer pump (500D) and an oil pump (260D).

Specifications	Model 500D	Model 260D
Capacity (mL)	507.38	266.05
Flow Range (mL/min)	Up to 204	Up to 107
Flow Accuracy	0.5% of setpoint	0.5% of setpoint
Pressure Range (psi)	[10-3750]	[10-7500]

The engineering sketch for the final setup can be seen in (Figure 7).

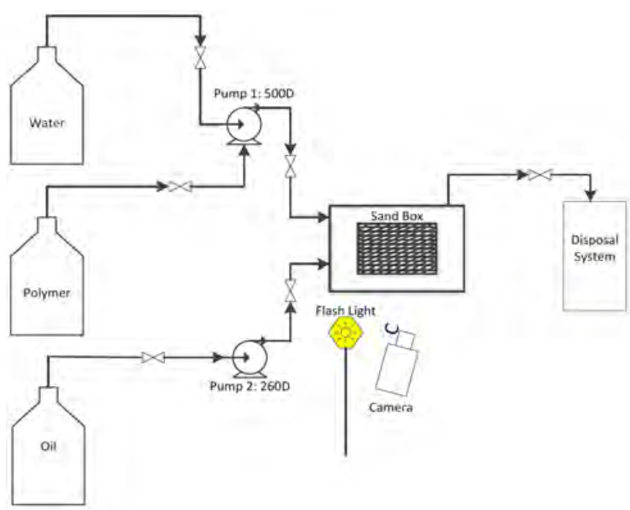

Figure 7—The final equipment setup diagram for the experiment.

Simulation Models

The simulation model used is to establish verification and validation of the experimental data. To accomplish this, we used commercial reservoir simulation software. We simulated the primary and secondary oil recovery processes with gravity and capillarity terms. Furthermore, the software is capable of running with a polymer option.

Simulation Model Description

We describe the dimensions, properties, and characteristics of the reservoir simulation grid. The model was constructed on a (50×1x50) Cartesian grid (I, J, K), with the K direction indexed downwards from top to bottom. The grid block sizes (0.2×0.25×0.2) cm are constant in all directions. They will represent the sandbox's exact dimensions (10×0.25×10) cm. For ease, the porosity and permeability maps were created in another numerical program and then incorporated into the simulator. The fracture was given a unique rock property that was not shared by the matrix (Figure 8).

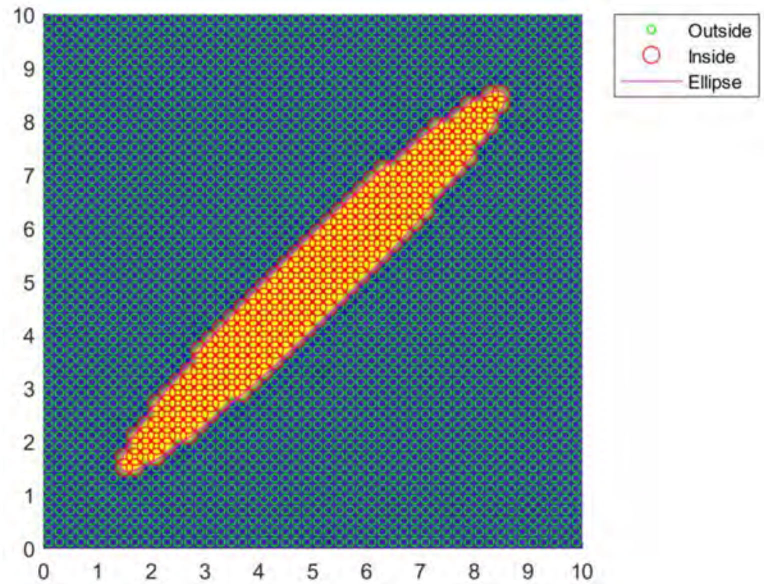

Figure 8—A generated image of a fracture as an ellipse inside a square, reflecting the matrix.

Likewise, permeability was achieved in a similar manner. The permeability values, on the other hand, were obtained through history-match iterations because permeability is best determined through core measurements. Knowing that we are dealing with unconsolidated sand makes estimating permeability values a little easier. Our estimate for the matrix was 4000 md, while the fracture was 35,000 md.

The Fluid Model and its Properties

Based on the polymer properties, we activated the polymer model and adjusted the polymer viscosity. Water has a viscosity of one mPa.s and a volume formation factor of one cm^3/cm^3. We assumed no water or oil compressibility, which is reasonable at low pressure. If the injected fluid is water, the viscosity of the polymer solution is 1.0 mPa.s. If the injected fluid is a polymer, the polymer solution has a viscosity of 150 mPa.s. The polymer concentration is 1000 ppm when the reference polymer concentration is 0.001 g/cc.

Rock Fluid Properties

Because we are dealing with water or polymer solution in a single-phase flow, relative permeability and capillary pressure are intuitive because there is no gas or oil in this system. As for two-phase flow systems, we estimated the relative permeability empirically using the saturation exponent provided by the Brooks-Corey power-law model(Baker et al., 2015). The relative permeability curves for the matrix are shown in Figure 9. Figure 10 shows the relative permeability curves in the fracture. The correspondent data were estimated and modified based on many similar cases found in the literature (Jin et al., 2004; Miller, 1983).

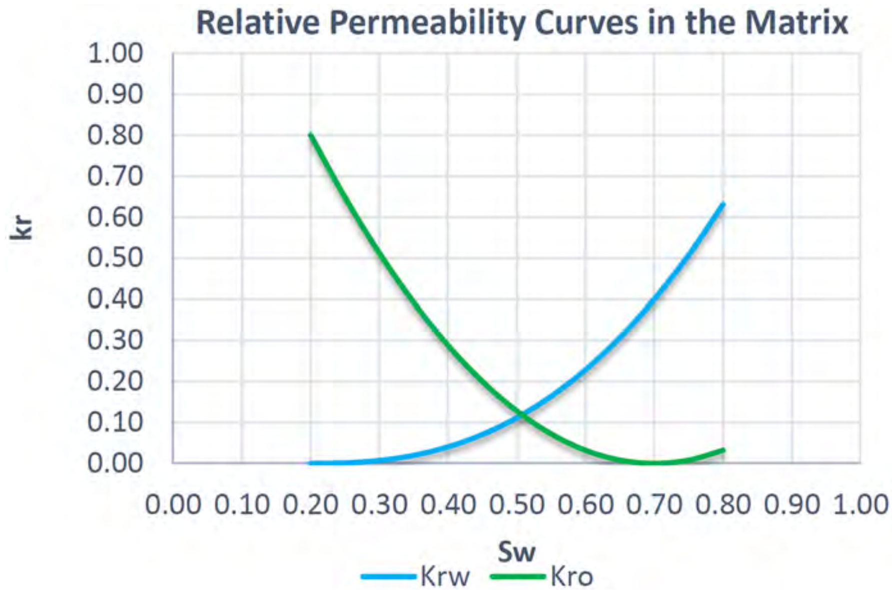

Figure 9—Plots of the matrix's relative permeability curves.

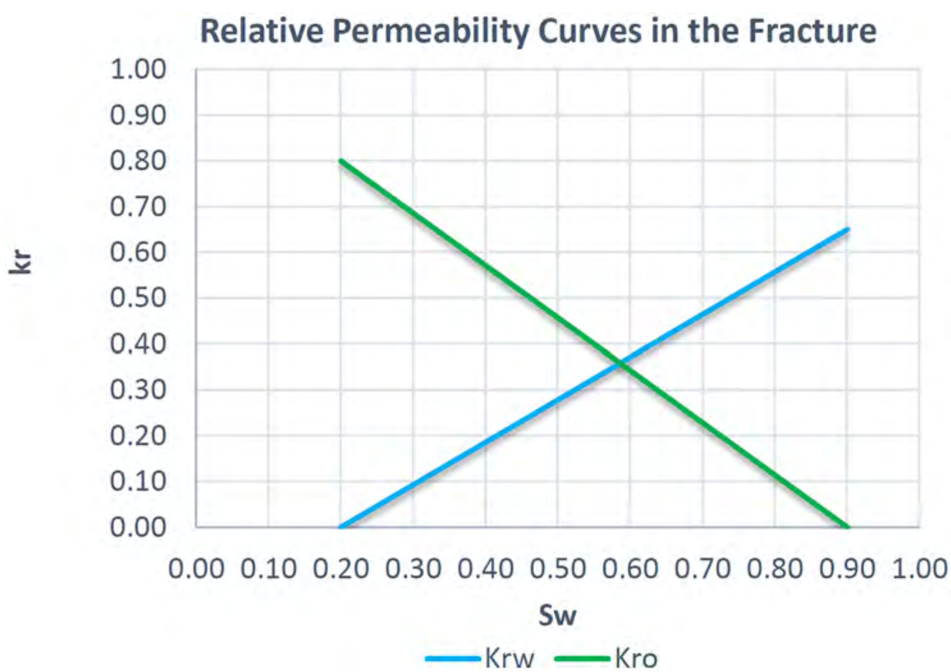

Figure 10—Plots of the fracture's relative permeability curves.

Where k_{rw} and k_{ro} represent the relative permeabilities of water and oil, respectively. S_w denotes the initial saturation of water.

Well and Recurrent Data

The wells were set after the initial conditions, and numerical controls were in place. Two wells were installed, one injector in the bottom left corner and one producer in the top right corner. Both run at the same flow rate, which corresponds to the pump's constant flow rate in the experiment (0.50 cc/min). Figure 11 depicts the porosity map of the constructed simulation model.

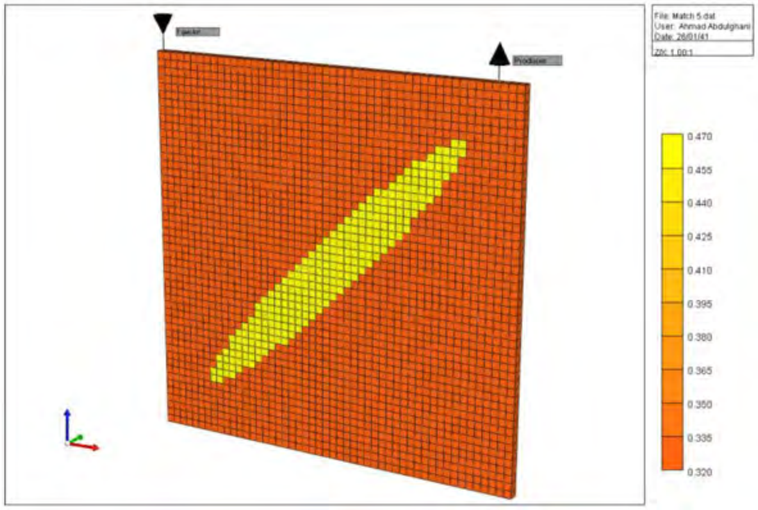

Figure 11—A depiction of the porosity map built-in the simulation model.

Results and Discussion

Single-Phase Flow Experiments

In the case of single-phase flow, we performed two baseline models. The first was when the displacing and displaced fluids were both water. However, we differentiated between the two by using tracer in the displacing fluid or the other way around. In the second scenario, we used a polymer to displace water in the sandbox.

Water Displacing Water

This case was carried out to establish a baseline. The total injection time for this experiment is approximately one hour to displace all of the sandbox fluid completely. The pressure drop began at about two psi and gradually decreased to around one psi when the interface encountered the fracture. The injected water (dyed in red) began to steadily displace the in-situ water inside the sandbox within the matrix media (Figure 12, **left**) until it encountered the fracture. The corresponding simulation results are shown in Figure 12, **right**.

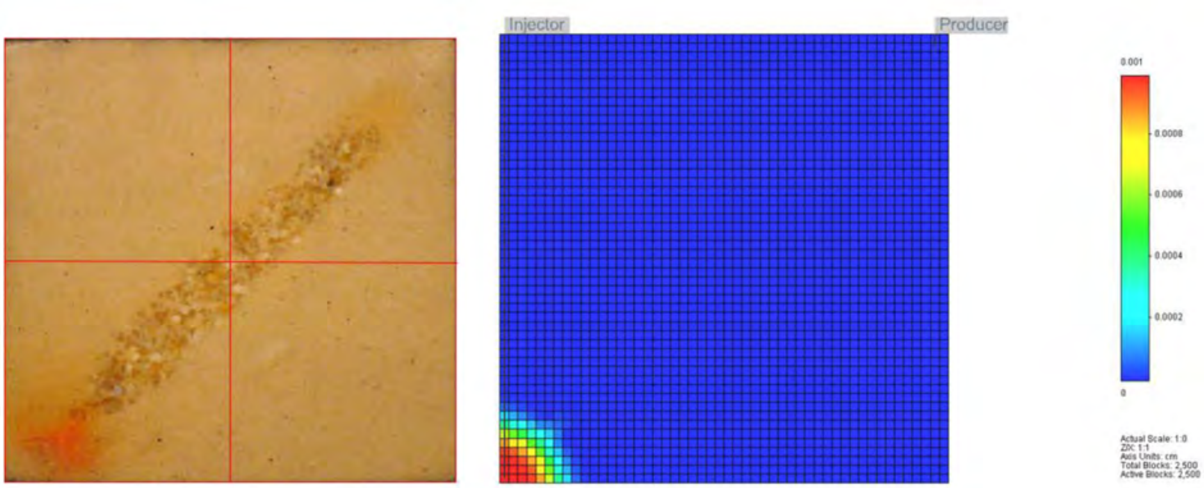

Figure 12—Two photos (experimental model on the left and simulation model on the right) depict the start of the water injection process (dyed in red) before encountering the fracture.

Once this occurred, the injected water began to divert to the fracture media until it was completely saturated with it. The water breakthrough occurred after 5 minutes of operation, leaving more than 65 percent of the initial fluid bypassed in the system (Figure 13). Later, the injected water gradually diffused to displace the bypassed water in the matrix media, which took approximately 55 minutes (Figure 14).

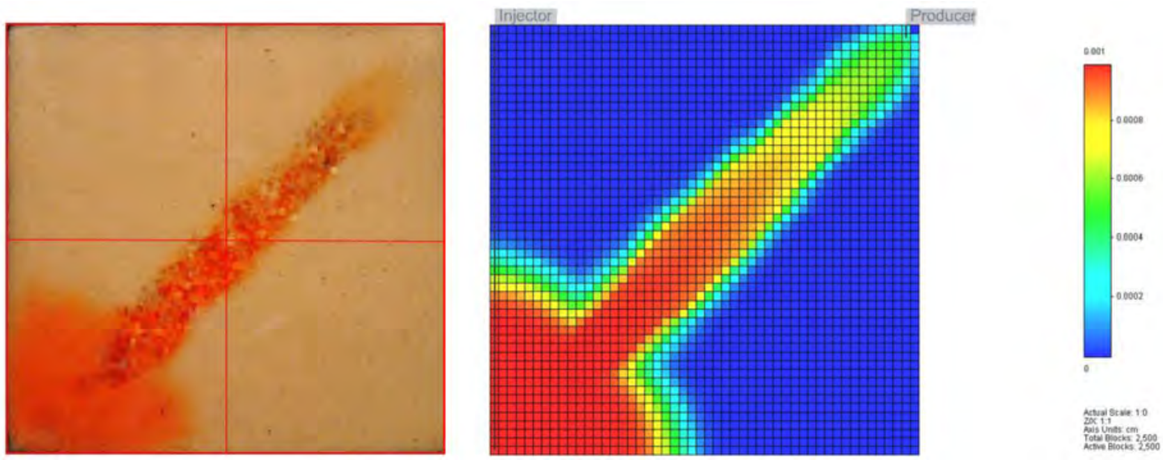

Figure 13—Two photos depicting how quickly water breakthroughs can occur after 5 minutes of running time.

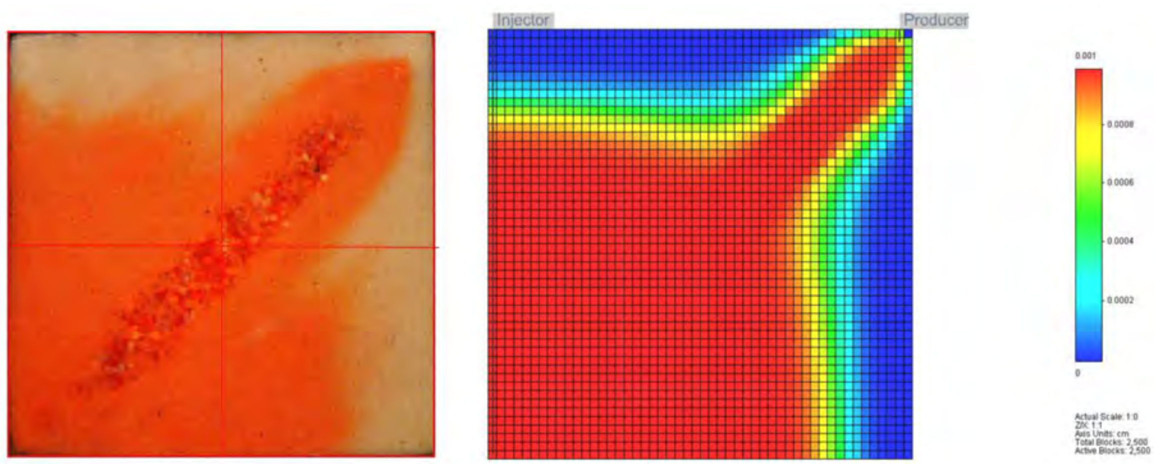

Figure 14—Two photos depict the displacement at half the experiment's duration.

The simulation model and the experimental model are matched. The permeability of the matrix, fracture, and injection flow rate are the most important controlling factors in the matching process. The simulation model reflects the displacement's behavior; thus, the actual fracture configuration is not visible. The color map depicts the saturation of the displacing fluid occupying the grid blocks, where deep blue is not yet occupied and dark red is fully saturated.

Capillarity is irrelevant in single-phase flow. Heterogeneity is, therefore, the dominant factor directing the flow. Since the fracture has the highest permeability value by several orders of magnitude, the injected water traversed the fracture faster with low crossflow, resulting in an insufficient volumetric sweep. At the reservoir time scale, the displacement could take weeks, months, or even years, leaving the operating companies dealing with water issues at the start of production.

Polymer Displacing Water

This case is a little different because we have water as the displaced fluid and polymer (dyed in red) as the displacing fluid. The experiment's total run time is less than 30 minutes, which is half of the run time in the first scenario. Furthermore, the pressure drop was reported to have increased by a factor of two.

Similarly, at a concentration of 1000 ppm, the polymer solution began to sweep locally within the matrix area prior to encountering the fracture (Figure 15). When it notices the fracture, it begins to move toward it but slowly. It continued like this for 20 minutes until the fracture healed. It then reverted to its original displacement behavior (Figure 16). It is worth noting that the polymer did not breakthrough as quickly as seen in the previous case. It was not detected in the production fluids until more than 90% of the water had been displaced. A better sweep was achieved in a relatively shorter time near the end of the experiment (Figure 17).

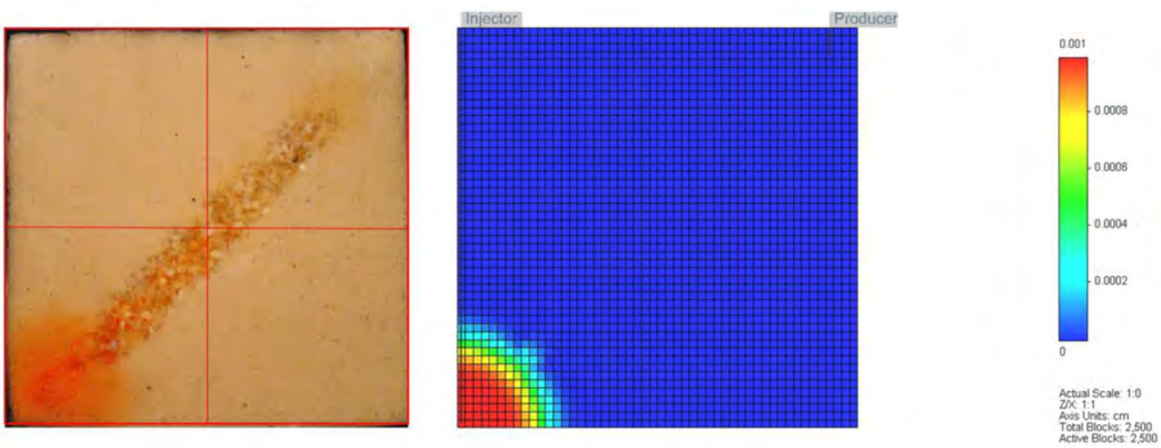

Figure 15—Two photos illustrate the start of the polymer flooding (in red) before encountering the fracture.

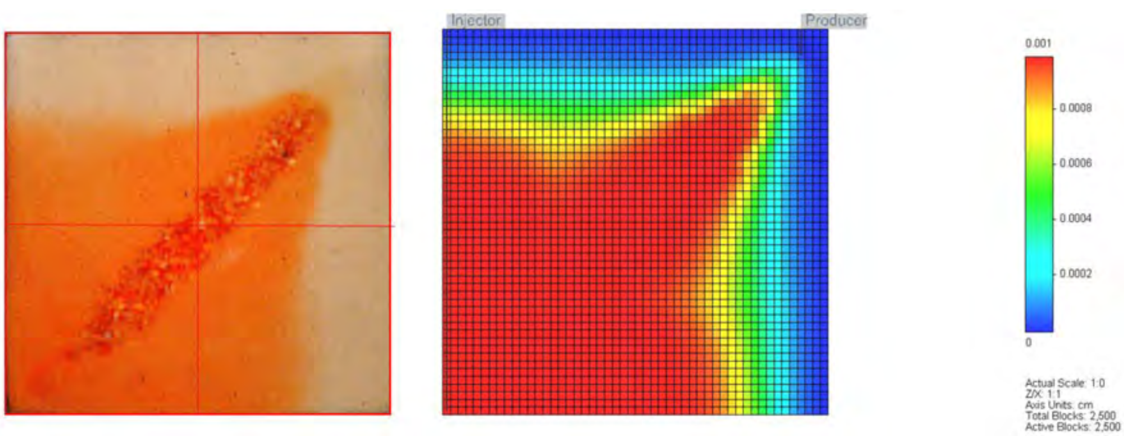

Figure 16—Two photos illustrate the polymer behavior during the displacement phase after 20 minutes of the run time.

The simulation model matched the experimental model well once more. The permeability of the matrix and the fracture, the injection flow rate, and, most importantly, the viscosity of the polymer solution are the most important controlling factors in the matching process.

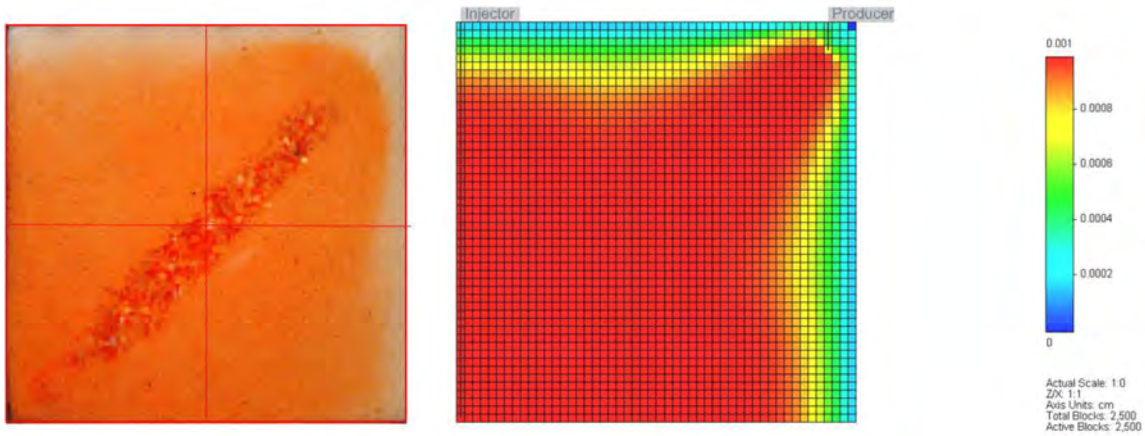

Figure 17—A composite of two photos depicts the polymer behavior near the end of the displacement.

Because the polymer solution has a higher viscosity, it has lower mobility. In this scenario, the mobility ratio will be less than one, resulting in a better sweep. Again, because we are dealing with a single-phase flow, capillarity has no effect. It is a matter of heterogeneity, and permeability is critical in directing the flow. The impact of permeability contrast, on the other hand, has been overcome by a polymer injection due to lower mobility. Despite the highest permeability value in the fracture, the injected polymer solution advanced more uniformly in the matrix and fracture regions.

In the sensitivity analysis, a higher polymer solution viscosity must be provided as a further step to improve the sweep. Higher viscosity, however, does not imply a better sweep. To that end, the total displacement run time and injection pressure will be increased. Because we are dealing with small-scale unconsolidated sand, these concerns may not be a major issue. Nonetheless, it is a significant decision in the oilfield business that must be made based on several factors.

Two-Phase Flow

We performed the experiments for two-phase flow after we had established the baselines for single-phase flow. Therefore, we repeated the same two scenarios. Still, rather than using water as a displaced fluid, we saturate the sandbox with oil this time, simulating reservoir fluids. Thus, the first experiment is performed when the displacing fluid is water, and the displaced fluid is oil. In the second scenario, we used a polymer solution to replace the oil in the sandbox.

Water Displacing Oil

This case is representative of the vast majority of waterflooding techniques used in water-wet reservoirs. The projection of this scenario will shed light on understanding the flow behavior in complex factors such as heterogeneity and capillarity. Therefore, this experiment was repeated several times with injection rates ranging from 0.5 to 20 cc/min. The most important ones are those on which we will concentrate our attention in this study. The takeaway of increasing the injected flow rate is to expedite the displacement process and monitor the impact of some key variables that take longer to appear.

Starting with an injection rate of 0.5 cc/min, the total injection time for this experiment is approximately 30 minutes to displace the oil within the majority of the matrix zone. Full matrix saturation took about two hours. The pressure drop fluctuated between one and two psi throughout the experiment, with no discernible change when the flow filled the matrix or was about to fill the fracture. This experiment yielded three obvious results. First, we noticed that the injected water (dyed in red) steadily displaced the oil inside the sandbox within the matrix media, gradually meandering to the production port.

Second, the interface between the fracture and the matrix has the highest velocity towards production. It appears to become saturated faster than any other area in the region except the area around the injector, where the actual flooding occurs. Water started to be produced in less than 8 minutes, which was less than a quarter of the time allotted for the experiment. Third, during the 30-minute experiment, the fracture media were not filled or saturated by water flooding (Figure 18).

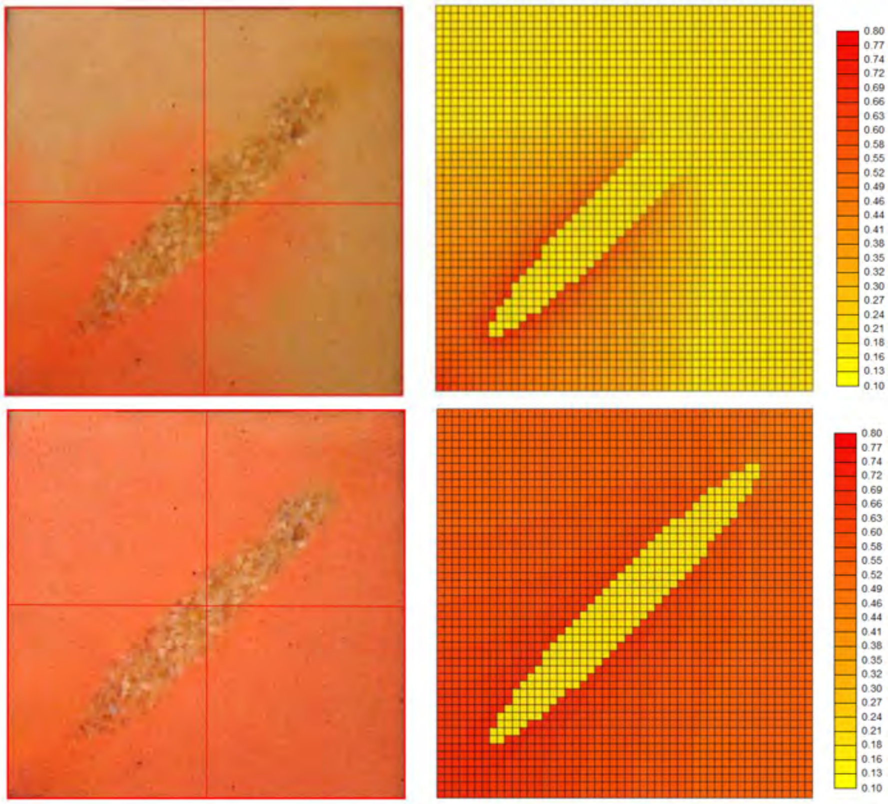

Figure 18—Snapshots of four photos show the behavior of the water flooding at 0.5 cc/min.

On the other hand, the simulation model matched the experimental model to the best of our ability as the number of variables increased. Furthermore, each controlling variable has a significant impact on the overall results. The most important controlling factors are the permeability of the matrix and the fracture, the injection flow rate, relative permeability, and capillary pressure. The simulation model in these figures reflects the displacement behavior in which the saturation map is shown. The color map depicts water saturation, with yellow representing initial water saturation and deep red demonstrating increased water saturation.

We discussed the behavior of waterflooding in fractured systems in the baseline water displacing water scenario. However, because we are dealing with two fluids, capillarity and mobility significantly influence this case (i.e., oil and water). Along with heterogeneity, we must account for capillary forces and mobility ratio.

At first, when capillarity and mobility had no effect in the baseline case, we observed that the flow preferred to channel to the high permeability media, which was the fracture. Adding another difficulty level, when two fluids come into contact, the mobility ratio has a minor impact on the flow behavior. Although the mobility ratio was 1.37, we observed a reasonably good sweep around the region. In the case of polymer displacing water, we observed a similar sweep displacement with a slow movement in the fracture media. Regardless of what happened to the fracture, a similar flow advancement is detected. What distinguishes this case is that there is no flow within the fracture, where capillarity comes into play.

We previously discussed the effect of interfacial tension, wettability, and pore size on capillary forces, and its geometry promotes capillary forces. Hence, in two immiscible fluids equilibria bounded by porous media, capillary pressure is the pressure contrast in the porous media between a non-wetting phase (i.e., oil) and a wetting phase (i.e., water). We also knew that smaller pore sizes exhibit higher capillarity than larger ones. Therefore, the observed flow behavior reflects a capillary flow. The pore volume within the matrix fills and becomes saturated faster than the pore volume within the fracture, which competes with viscous forces controlled by permeability. The significant difference in capillary forces at 0.5 cc/min versus 30 minutes was insufficient to induce flow in the fracture.

However, after 10 minutes of experimentation, we observed flow in the fracture at a 2.0 cc/min injection rate. Experimenting with different flow rates confirms our hypothesis. Figure 19 depicts the injection rates after 10 minutes of testing at 20 cc/min.

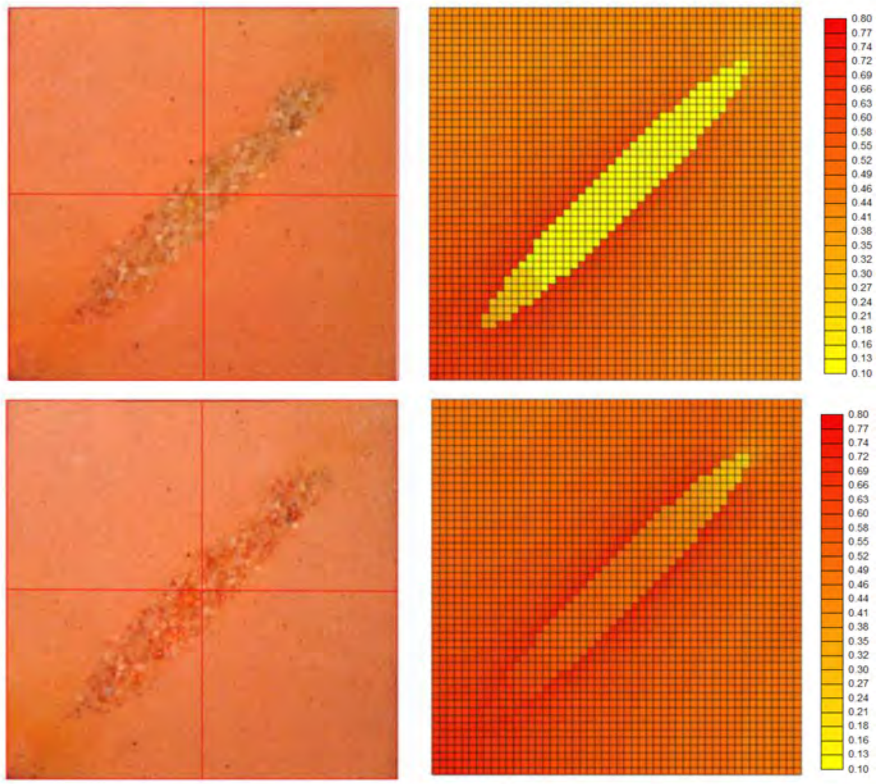

Figure 19—Four photos show that water flooding started saturating the fractured media at a 20 cc/min injection rate.

Polymer Displacing Oil

The impact of the polymer flooding in water-wet capillarity dominant heterogeneous medium aids in understanding flow behavior in the presence of complex factors such as heterogeneity, mobility ratio, and capillarity. Starting with an injection rate of 0.5 cc/min, the total injection time for this experiment was approximately 45 minutes to displace most of the oil within the porous media, which is longer than the water flooding. More than a double increase in pressure drop was consistently reported, between four and five psi. A similar polymer solution with a concentration of 1000 ppm was prepared and used. Technically, we observed fluid displacement behavior similar to that observed in the polymer displacing water baseline case. The significant difference is that the flow advancement we previously observed in the fracture is now seen as receding (Figure 20).

The simulation model best matches the experimental model with the same parameters as in the previous cases. The most controlling factors in the matching process are the permeability of the matrix and the fracture, the injection flow rate, polymer viscosity, relative permeability, and capillary pressure curves for the matrix and the fracture.

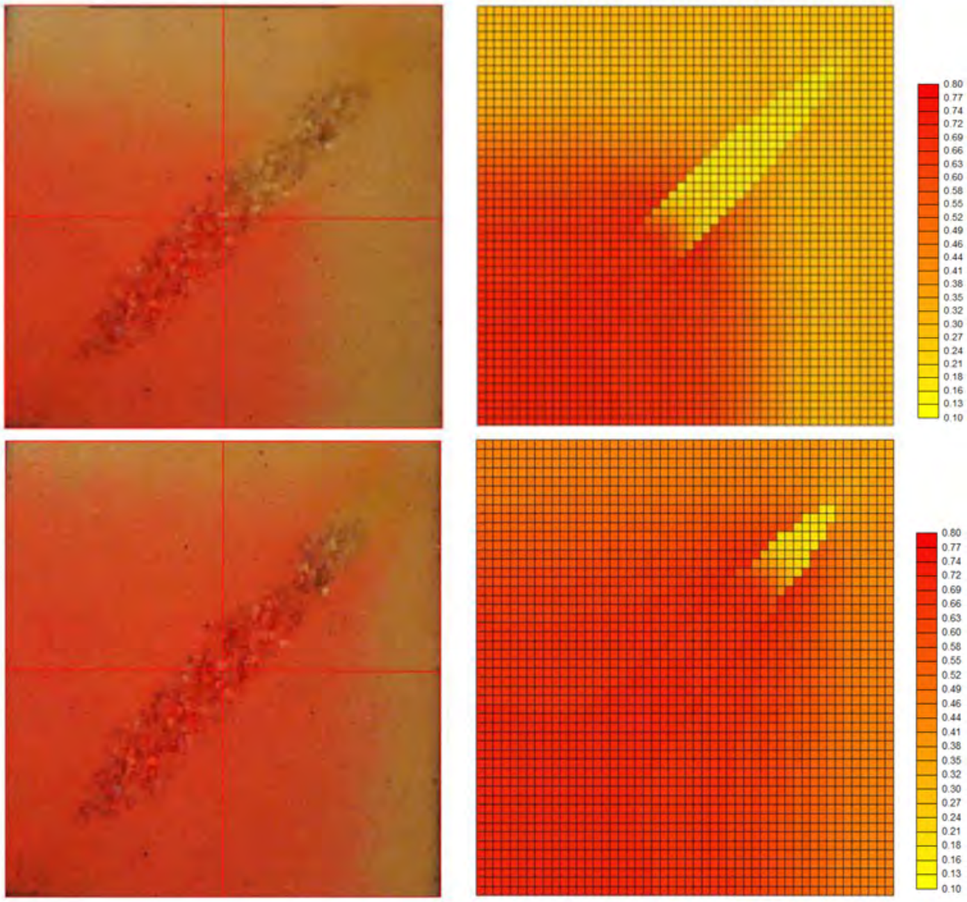

Figure 20—Snapshots of the polymer flooding displacement taken from the beginning to the end of the experiment.

Again, in these figures, the simulation model reflects the displacement behavior in which the saturation maps are shown. The saturation of the displaced fluid occupying the grid blocks is depicted by the color map, with deep red saturated with oil and deep blue saturated with a polymer solution.

In the polymer displacing water scenario, we established a baseline of polymer flooding in fractured systems, and we realized the impact of capillarity in the water flooding displacing oil scenario. Capillarity and mobility ratio are the two most significant contributors to the overall sweep. As the polymer solution has a higher viscosity and it thus has different mobility than oil. The mobility ratio, in this scenario, will be less than one, resulting in a better sweep than water flooding. However, capillarity has an actual influence as we are dealing with two phases with different grain sizes. In addition to the heterogeneity, strong capillary forces contribute to the overall flow behavior. Capillarity is responsible for the withdrawal-like flow behavior observed in fracture media rather than the advancement observed in single-phase flow.

Smaller pore sizes have greater capillarity than larger pore sizes. As a result, the observed flow divergence behavior is consistent with a dominant capillary flow. Regardless of permeability, the pore volume within the matrix is filled and saturated faster than the one within the fracture.

Conclusion

This study investigated key physical elements that significantly impact the overall fluid flow behavior in porous media. The work discussed the impact of capillarity in heterogeneous reservoirs. The goals of designing, fabricating, and testing a 2D lab-scale sandbox model of a fractured porous medium with injection and production ports were met. The experiment was carried out for single-phase and two-phase flow scenarios with water or polymer injection. The displacement results were evaluated, verified, and validated using reservoir simulation software.

Two scenarios were considered baseline models in the case of single-phase flow because the controlling variables are limited and governed, which helped distinguish the contrast from the later cases. The first was when the displacing and displaced fluids were both water. In the second case, the displacing fluid was a polymer. Water prefers to channel through high permeable streaks with minimal crossflow, resulting in a deficient volumetric sweep and largely bypassed zones when water injection is used in a fractured water-wet formation. The investigation of two-phase flow, on the other hand, was carried out using the same procedures but with oil as the displacing fluid instead of water. During water flooding, due to the strong capillarity contrast between the matrix and fracture, flow divergence was found to be faster in the matrix media. The pore volume within the matrix was flooded faster than within the fracture, regardless of its permeability, depending on the injection rate. On the other hand, polymer flooding demonstrated a better volumetric sweep in all scenarios in both one-phase and two-phase flow. It outperformed water flooding, exhibited a delay in water breakthrough, and improved volumetric sweep even when capillarity was involved.

Nomenclature

CEOR	Chemical Enhanced Oil Recovery
EOR	Enhanced Oil Recovery
NFR	Naturally Fractured Reservoir
PF	Polymer Flooding
ppm	Parts Per Million
RF	Recovery Factor
SAGP	Steam and Gas Push
TDS	Total Dissolved Solids
WF	Waterflooding

References

Al-Nakhli, A. R., Bataweel, M., Almohsin, A., & Al-Badairy, H. (2016). A Breakthrough Water Shutoff System for Super-K Zones in Carbonate Ghawwar Field: Adsorption and Polymer System. Society of Petroleum Engineers - Abu Dhabi International Petroleum Exhibition and Conference 2016.

Albattat, R., & Hoteit, H. (2021). A semi-analytical approach to model drilling fluid leakage into fractured formation. *Rheologica Acta* 2021 **60**:6, 60(6), 353–370. https://doi.org/10.1007/S00397-021-01275-3

Almohsin, A., Huang, J., Karadkar, P., & Bataweel, M. (2017, July 9). Nanosilica Based Fluid System for Water Shut-Off. *OnePetro*. Retrieved from http://onepetro.org/WPCONGRESS/proceedings-pdf/WPC22/4-WPC22/D043S006R004/1254627/wpc-22-0468.pdf

Aublinger, C. (2015). Shape Factor Estimation and WAG Simulation in Naturally Fractured Reservoirs. The University of Leoben.

Bailey, B., Crabtree, M., Elphick, J., Kuchuk, F., Romano, C., & Roodhart, L. (2000). Water Control. *Oilfield Review*, 30–51.

Baker, R., Yarranton, H., & Jensen, J. (2015). Practical Reservoir Engineering and Characterization. Elsevier Inc. https://doi.org/10.1016/C2011-0-05566-7

Burchette, T. (2012). Carbonate Rocks and Petroleum Reservoirs: A Geological Perspective From the Industry. *Geological Society Special Publication*, **370**(1), 17–37. https://doi.org/10.1144/SP370.14

Donaldson, E., George, C., & Yen, T. (1985). Enhanced Oil Recovery I, Fundamentals and Analyses. Elsevier Science Publishers.

Fanchi, J. R. (2006). Petroleum Engineering Handbook, Volume I: General Engineering. (Lake L., Ed.), Petroleum Engineering Handbook (Vol. **I**). Texas: Society of Petroleum Engineers.

Glasbergen, G., Abu-Shiekah, I., Balushi, S., & Van Wunnik, J. (2014). Conformance Control Treatments for Water and Chemical Flooding: Material Screening and Design. Society of Petroleum Engineers - SPE EOR Conference at Oil and Gas West Asia 2014: Driving Integrated and Innovative EOR, 83–92.

Goudarzi, A., Almohsin, A., Varavei, A., Delshad, M., Bai, B., & Sepehrnoori, K. (2014). New Experiments and Models for Conformance Control Microgels. Proceedings - SPE Symposium on Improved Oil Recovery, **3**, 1752–1768.

He, X., Sinan, M., Kwak, H., & Hoteit, H. (2021). A corrected cubic law for single-phase laminar flow through rough-walled fractures. *Advances in Water Resources*, **154**, 103984. https://doi.org/10.1016/J.ADVWATRES.2021.103984

He, X., Santoso, R., Zhu, W., Hoteit, H., AlSinan, M. M., & Kwak, H. T. (2021, November). Coupled Flow-Normal-Shear Influence on Fracture Permeability: Analysis and Modeling. ARMA/DGS/SEG 2nd International Geomechanics Symposium.

Hoteit, H. (2013). Modeling diffusion and gas-oil mass transfer in fractured reservoirs. *Journal of Petroleum Science and Engineering*, **105**, 1–17. https://doi.org/10.1016/j.petrol.2013.03.007

Hoteit, H., & Firoozabadi, A. (2008). Numerical modeling of two-phase flow in heterogeneous permeable media with different capillarity pressures. *Advances in Water Resources*, **31**(1), 56–73. https://doi.org/10.1016/j.advwatres.2007.06.006

Hoteit, H., Alexis, D., Adepoju, O. O., Chawathe, A., & Malik, T. (2016). Numerical and experimental investigation of polymer-induced resistance to flow in reservoirs undergoing a chemical flood. In Proceedings - SPE Annual Technical Conference and Exhibition (Vol. 2016-Janua). Society of Petroleum Engineers (SPE). https://doi.org/10.2118/181720-ms

Jin, G., Patzek, T., & Silin, D. (2004). Direct Prediction of the Absolute Permeability of Unconsolidated and Consolidated Reservoir Rock. Proceedings - SPE Annual Technical Conference and Exhibition, 1287–1301.

Lake, L., Johns, R., Rossen, W., & Pope, G. (2014). Fundamentals of Enhanced Oil Recovery.

Lyons, W. C., Plisga, G. J., & Lorenz, M. D. (2015). Standard Handbook of Petroleum and Natural Gas Engineering. Standard Handbook of Petroleum and Natural Gas Engineering (Third). Gulf Professional Publishing. https://doi.org/10.1016/C2010-0-64695-5

Miller, M. (1983). Effect of Temperature on Oil-Water Relative Permeabilities of Unconsolidated and Consolidated Sands. Sandford, California.

Muggeridge, A., Cockin, A., Webb, K., Frampton, H., Collins, I., Moulds, T., & Salino, P. (2014). Recovery rates, enhanced oil recovery and technological limits. *Philosophical Transactions of the Royal Society A: Mathematical, Physical and Engineering Sciences*, **372**(2006). https://doi.org/10.1098/rsta.2012.0320

Narr, W., Schechter, D., & Thompson, L. (2006). Naturally Fractured Reservoir Characterization. Richardson: Society of Petroleum Engineers. Retrieved from https://store.spe.org/Naturally-Fractured-Reservoir-Characterization-P40.aspx

Nelson, R. A. (2001). Geologic Analysis of Naturally Fractured Reservoirs. Geologic Analysis of Naturally Fractured Reservoirs. *Gulf Professional Pub.* https://doi.org/10.1016/b978-0-88415-317-7.x5000-3

Da Prat, G. (1990). Well Test Analysis for Fractured Reservoir Evaluation. Elsevier.

Satter, A., & Iqbal, G. (2016). Reservoir Engineering: The Fundamentals, Simulation, and Management of Conventional and Unconventional Recoveries. *Reservoir Engineering. Elsevier*. https://doi.org/10.1016/B978-0-12-800219-3.00003-6

Schlumberger Limited. (2008). Carbonate Reservoirs: Meeting Unique Challenges to Maximize Recovery. Schlumberger. Schlumberger.

Selley, R. (1985). Elements of Petroleum Geology. *Elements of Petroleum Geology.*, **507**.

Sheng, J. (2011). Modern Chemical Enhanced Oil Recovery: Theory and Practice. Gulf Professional Publishing (First). Elsevier. https://doi.org/10.1016/B978-1-85617-745-0.00001-2

Shepherd, M. (2009). Factors Influencing Recovery From Oil and Gas Fields. *Oil Field Production Geology: AAPG Memoir* **91**, 37–46. https://doi.org/10.1306/13161187M913372

Sugar, A., Torrealba, V., Buttner, U., & Hoteit, H. (2021). Assessment of Polymer-Induced Clogging Using Microfluidics. *SPE Journal*, **26**(06), 3793–3804. https://doi.org/10.2118/201626-PA

Terry, R., & Rogers, B. (2015). Applied Petroleum Reservoir Engineering (Third Edit). Westford, Massachusetts: Pearson Education, Inc.

Warren, J. E., & Root, P. J. (1963). The Behavior of Naturally Fractured Reservoirs. *Society of Petroleum Engineers Journal*, **3**(03), 245–255. https://doi.org/10.2118/426-pa